JOURNAL OF AGRICULTURAL AND FOOD CHEMISTRY

Article

pubs.acs.org/JAFC

Nanoparticles Synthesized from Soy Protein: Preparation, Characterization, and Application for Nutraceutical Encapsulation

Zi Teng, Yangchao Luo, and Qin Wang*

Department of Nutrition and Food Science, University of Maryland, 0112 Skinner Building, College Park, Maryland 20742, United States

ABSTRACT: Nanoparticles were synthesized from soy protein, one of the most abundant and widely utilized plant proteins, for nutraceutical and drug encapsulation. The preparation process consisted of dispersion, desolvation, drug incorporation, cross-linking, and evaporation. The role of each procedure in the formation of nanoparticles was systematically investigated by means of particle size, size distribution, and zeta potential as well as morphology observation. Curcumin as a model drug was encapsulated successfully into the nanoparticles, evidenced by Fourier transform infrared spectroscopy and X-ray diffraction patterns. The average size of the curcumin-loaded nanoparticles was 220.1 to 286.7 nm, and their zeta potential was around −36 mV. The highest encapsulation efficiency and loading efficiency achieved were 97.2% and 2.7%, respectively. The release of curcumin in phosphate buffer saline followed a biphasic pattern. Possible mechanisms of the formation of soy protein nanoparticles as well as the incorporation of curcumin were discussed based on the data obtained from this study.

KEYWORDS: *Soy protein, Nanoparticles, Curcumin, Encapsulation, Controlled release*

INTRODUCTION

Biopolymer-based nanoparticles have gained increasing interest as delivering systems for drug and nutraceuticals in the past few decades.[1−3] Their subcellular size provides several advantages such as prolonged gastrointestinal residence,[4] better tissue penetration, and superior cellular uptake.[5] Besides, they exhibit low toxicity owing to their biodegradability and nonantigenic property.[6] Proteins as amphiphilic biopolymers are deemed as ideal materials for preparing nanoparticles because they interact well with both the drug and solvent.[2] By far, drug-loaded nanoparticles have been synthesized successfully from various proteins,[2,6−8] including both water-soluble (bovine or human serum albumin) and insoluble proteins (zein, gliadin, etc.). These nanoscaled systems exhibited various advantages, such as improved solubility, controlled release property and enhanced bioavailability of encapsulated nutraceuticals. However, several limitations hindered their applications in pharmaceutical and food industry. For instance, albumins contain a relatively low content of hydrophobic amino acids, and they incorporate drugs majorly via electrostatic attraction or hydrogen bonds.[9,10] Therefore, they are less capable in encapsulating highly hydrophobic drugs that are not charged and form few hydrogen bonds. In contrast, nanoparticles prepared with zein or gliadin performed satisfyingly in incorporating hydrophobic chemicals,[7,11] but their low content in hydrophilic and charged amino acids resulted in a limited solubility in aqueous environment, unless a considerable amount of polysaccharides or surfactants was added.[11,12]

Soybean (*Glycine max L.*) is currently one of the most abundant sources of plant proteins. The enriched form of soy protein, known as soy protein isolate (SPI), has been reported to exhibit high nutritional values and desirable functionalities, and its wide application as a food ingredient has been well documented.[13−15] Besides, SPI possesses a balanced composition of nonpolar, polar, and charged amino acids,[13] thus being able to incorporate drugs with its various functional groups. The major components of SPI were glycinin (MW = 360,000, approximate 60%) and β-conglycinin (MW = 180,000, approximate 40%).[16] In aqueous environment, these components exist majorly as globular molecules consisting of a hydrophilic shell and a hydrophobic kernel, together with a certain amount of small water-soluble aggregates.[17,18] Upon the addition of desolvant or cross-linking agents, SPI molecules continue to aggregate and form various structures, such as microspheres,[19] hydrogels,[15] and polymer blends.[14,20] However, to the best of our knowledge, there has been no systematic report by now on the fabrication of nanoparticles with SPI.

In this study, nanoparticles were synthesized with SPI by adopting a desolvation technique followed by glutaraldehyde cross-linking.[6] The nanoparticles were characterized by the particle size, size distribution, count rate, zeta potential, and morphology. The effects of each step of preparation (i.e., desolvation, cross-linking, and evaporation) on the above parameters were investigated systematically. Curcumin (diferuloylmethane) was selected as a model drug for evaluating the encapsulating property of SPI nanoparticles. The Fourier transform infrared (FT-IR) spectra, X-ray diffraction (XRD) pattern, encapsulation efficiency, and releasing profile of the curcumin-loaded particles were measured. Finally, a possible mechanism of the formation of blank and curcumin-loaded SPI nanoparticles was proposed based on the data obtained in this study.

Received: December 20, 2011
Revised: February 13, 2012
Accepted: February 20, 2012
Published: February 21, 2012

dx.doi.org/10.1021/jf205238x | *J. Agric. Food Chem.* 2012, 60, 2712−2720

MATERIALS AND METHODS

Materials. Prolia 200/70 Defatted Soy Flour was a sample donated by Cargill Inc., Cedar Rapids, IA, USA. The soy flour contained 54% protein (dry basis) and less than 1% oil. Curcumin (95% pure) was purchased from Sigma-Aldrich (St. Louis, MO, USA). All other chemicals (glutaraldehyde, Tween 20, phosphate buffer saline, etc.) were of analytical grade.

Preparation of SPI. SPI was prepared following an isoelectric precipitation method.[21] The defatted soy flour was suspended in 15-fold of deionized water with mild stirring, and the pH of the suspension was adjusted to 8.0 with 1 mol/L NaOH. After 1 h of extraction, the dispersion was centrifuged at 10,000*g* for 15 min. The supernatant was acidified with 1 mol/L HCl to pH 4.5 and centrifuged under the same condition. The precipitate was redispersed in water, adjusted to pH 7.5 with 1 mol/L NaOH, dialyzed against deionized water for 24 h and then lyophilized. The moisture content of the final product was less than 5%, while the protein content was 90% as determined by Bradford assay with bovine serum albumin as the standard protein.

Preparation of Blank Nanoparticles with SPI. Nanoparticles were prepared with freshly prepared SPI following a desolvation method[6] with modifications. SPI was dissolved in deionized water at concentrations of 4 to 60 mg/mL and equilibrated for 1 h at room temperature. Desolvating agent (ethanol) was added dropwise into the dispersion. The concentrations of SPI and ethanol after mixing ranged from 4−12 mg/mL and 0−80%, respectively. After 15 min of equilibration, glutaraldehyde (25 mg/mL aqueous solution) was added as a cross-linker. The amount of glutaraldehyde was calculated as below. The average molecular weight of SPI (288,000) was estimated based on its composition, which was described in the introduction, while the lysine content of SPI was obtained from previous literature.[13] These values, together with the fact that one glutaraldehyde molecule reacted with two lysine residuals, gave the amount of glutaraldehyde required for stoichiometric cross-linking, which was 28 μg/mg SPI or 77 mol/mol SPI. This ratio was defined as 100% glutaraldehyde equivalent, and the amount of added glutaraldehyde ranged from 0% to 150% calculated based on this value in our study. The purpose of adding more than 100% equivalent of glutaraldehyde was to achieve a higher reaction rate.[6,22] After 16 h of cross-linking reaction at room temperature, 3-fold of aqueous ethanol was added to dilute the dispersion without changing its ethanol/water ratio. Thereafter, rotary evaporation was applied using a Buchi Rotavapor RII at 30 °C (BUCHI Labortechnik AG, Flawil, Switzerland) to remove ethanol, which was then replaced with the same volume of deionized water. The resultant dispersion, containing less than 10% ethanol, was centrifuged at 10,000*g* for 15 min to remove large aggregates. The percentage of protein in the supernatant was higher than 95%, as determined by Bradford assay. The supernatant was either lyophilized or stored at 4 °C for subsequent assays.

Preparation of Curcumin-Loaded SPI Nanoparticles. The encapsulation of curcumin into SPI nanoparticles was achieved as described below. Typically, SPI (60 mg/mL) was suspended in deionized water, while curcumin (3 mg/mL) was dissolved in ethanol as a stock solution. After 1 h of equilibration, pure ethanol was added dropwise to the SPI dispersion to the concentration of approximately 60%. Curcumin stock solution was then added dropwise to attain a curcumin/SPI ratio of 1:20, 1:50, or 1:100 (w/w). Additional ethanol was introduced finally to achieve an ethanol/water ratio of 80:20 (v/v). The dispersion was then cross-linked, diluted, evaporated, rediluted, and centrifuged as described in the above section. The supernatant obtained after centrifugation was stored at 4 °C for subsequent analyses.

Determination of Particle Sizes and Count Rates. The dispersions of both blank and curcumin-loaded SPI nanoparticles were analyzed at different preparation stages. The particle size as well as the count rate was determined by dynamic laser scattering (DLS) using a BI-200 SM Goniometer Version 2 (Brookhaven Instrument Corp., Holtsville, NY, USA) equipped with a 35 mW He−Ne laser beam at a wavelength of 637 nm and a scattering angle of 90°.[6] The average size and size distribution were calculated by using the BIC Dynamic Scattering Software (Brookhaven Instrument Corp., Holtsville, NY, USA) based on the intensity of the scattered light. The reflective index and viscosity of water/ethanol mixtures with different volume ratios were applied for obtaining accurate results. In order to obtain comparable count rates, the samples were not diluted, and the power of laser was fixed at 10 mW. All of the analyses were conducted at 25 °C for 1 min.

Determination of Zeta Potential of the Nanoparticles. During the preparation process, the nanoparticle dispersions were measured for their electrophoretic mobility by laser Doppler velocimetry using a Nano ZS90 Zetasizer and compatible fold capillary cuvettes provided by Malvern Inc. (Malvern, UK). The electrophoretic mobility of each sample was measured three times, and at least 12 runs were performed in each measurement. The data were then converted to zeta potentials using the Smoluchowski model.

FT-IR Study of the Nanoparticles. The blank and curcumin-loaded nanoparticles were lyophilized before FT-IR analysis. Each sample (3 mg) was loaded on a Jasco FT/IR 4100 spectrometer (Jasco Inc., Easton, MD, USA). The infrared spectra were collected from the wavenumber of 700 to 4000 cm^{-1} at a resolution of 4 cm^{-1}. Each sample was subjected to 60 repeated scans. The spectra were averaged and smoothed, and their baselines were calibrated with the Spectra Manager software (Jasco Inc., Easton, MD, USA).

X-ray Diffraction (XRD) Analysis. The X-ray diffraction (XRD) patterns of SPI, curcumin, their physical mixture (curcumin: SPI = 1:40, w/w) and SPI-encapsulated curcumin were recorded on a Bruker D8-Advance Diffractometer (Bruker AXS Inc., Madison, WI, USA) with backgroundless sample holders. The working parameters were voltage of 40 kV, current of 40 mA, and scanning rate of 3 min^{-1}.

Scanning Electronic Microscopy (SEM) Analysis. SEM was performed to examine the morphological structure of blank and curcumin-loaded nanoparticles. Dispersions of particles were diluted with aqueous ethanol, so that the ethanol concentration was unchanged, while the protein concentration was approximately 0.5 mg/mL. Fifty microliters of the dispersion was cast-dried on an aluminum pan, which was cut into an appropriate size. The pan was adhered to a 1 inch specimen stub with conductive carbon tapes (Electron Microscopy Sciences, Ft. Washington, PA, USA). The stub was then coated with a thin layer (<20 nm) of conductive gold and platinum using a sputter coater (Hummer XP, Anatech, CA, USA) before observation under SEM (Hitachi SU-70 Pleasanton, CA, USA). Representative images were reported.

Determination of Encapsulation Efficiency (EE) and Loading Efficiency (LE). The encapsulation efficiency, defined as the percentage of curcumin encapsulated in the suspended protein nanoparticles, was estimated as below. After the centrifugation mentioned in the nanoparticle preparation sections, both the precipitate and supernatant (defined as the primary supernatant) were collected. The precipitate was extracted in 5 mL of ethanol with mild stirring for 5 min, after which the suspension was centrifuged at 9,000*g* and 20 °C for 5 min to remove protein aggregates. The resultant supernatant (defined as the secondary supernatant) was subjected to spectrophotometric analysis at 426 nm with a DU-730 UV/vis spectrophotometer (Beckman Coulter Inc., Fullerton, CA, USA). The absorbance was converted to curcumin concentration based on the established standard curve (R^2 = 0.9991). Meanwhile, the primary supernatant was decanted into a Macrosep centrifuge tube (Pall Corp., Ann Harbor, MI, USA) with a built-in filtering membrane (MW cutoff = 10,000) with appropriate dilution.[23] After centrifugation at 5,000*g* and 20 °C for 30 min, the free (nonencapsulated) curcumin permeated the membrane and was quantified spectrophotometrically. The EE of the samples were calculated with the following equation:

$$\mathrm{EE}(\%) = 100 - \frac{\text{precipitated curcumin} + \text{free curcumin}}{\text{total curcumin}} \times 100$$

After the aforementioned centrifugation, the nonpermeable part of the dispersion was collected and lyophilized. The mass of dry nanoparticles was measured, and the loading efficiency (LE) was calculated

as the mass ratio of encapsulated curcumin to the obtained nanoparticles.

Release of Curcumin in Phosphate Buffer Saline (PBS). Five milligrams of lyophilized nanoparticles was weighed and dispersed in 10 mL of the release medium (PBS, pH 7.5 with 0.5% Tween 20). The dispersion was incubated at 37 °C with mild shaking on a Multi-Purpose Rotator/Rocker (Scientific Industries Inc., NY, USA) for 0.5 to 8 h. The mixture was centrifuged at 51,500*g* and 20 °C for 15 min, after which over 90% of the nanoparticles were precipitated (preliminary data not shown). The supernatant containing released curcumin was analyzed spectrophotometrically as mentioned before, using a calibration curve established in curcumin/Tween 20/PBS system (R^2 = 0.9993). The precipitate was disposed, and a fresh dispersion was then made for another measurement. The kinetic release profile of curcumin was plotted as a function of time.

Statistics. All measurements were performed in triplicates. The experimental results obtained were expressed as means ± standard error. Data were analyzed by analysis of variance ($p < 0.05$) using the Origin 7.5 software (OriginLab Corp., MA, USA).

RESULTS AND DISCUSSION

Effect of the Desolvation Process. Figure 1A,B showed the particle size and zeta potential of SPI dispersions, respectively, as influenced by ethanol and protein concentrations. No glutaraldehyde addition nor centrifugation was undertaken at this stage. The effective size of SPI dispersion in pure water was around 320 nm, which was in accordance with the previous literature.[24,25] As the concentration of ethanol increased to 30−40% (depending on the final protein concentration), the particle sizes increased gradually before reaching a peak. This was probably because that high ethanol content favored the exposure and interaction of the hydrophobic chains in protein molecules, which led to the formation of aggregates.[18,26] Similar behavior was reported in the study on human serum albumin (HSA) nanoparticles.[6] Besides, the peak particle size averaged at 606 and 862 nm at SPI concentrations of 4 mg/mL and 12 mg/mL, respectively. This difference might be attributed to the fact that higher protein concentration favored the collision and aggregation of protein molecules.[27] As the percentage of ethanol increased to 80%, the particle sizes decreased significantly, and smaller average particle sizes were observed at higher protein concentrations (Figure 1A). The decrease in average size at high ethanol concentrations was unexpected and has not been reported in previous literatures. It could be attributed to either breakdown of larger aggregates or the extensive formation of smaller ones. To elucidate the behavior of soy protein at high ethanol levels, the size distribution and count rate of the dispersion were analyzed and presented below.

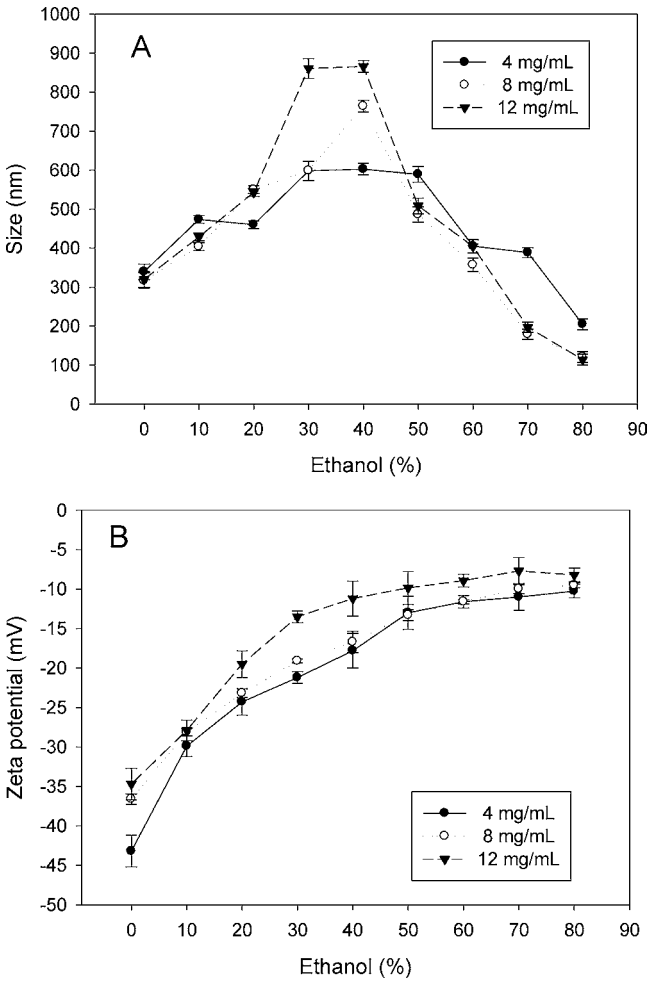

Figure 1. Effect of ethanol and protein concentrations on the size (A) and zeta potential (B) of soy protein isolate nanoparticles.

Figure 2A,B showed the size distributions of two SPI dispersions at the same protein concentration (i.e., 8 mg/mL) but different ethanol percentages (i.e., 0% for 2A and 80% for 2B). Two groups, one corresponding to small particles (50−200 nm, similarly hereinafter) and the other representing large aggregates (500−1000 nm, similarly hereinafter), were observed in both diagrams. Compared with the SPI dispersed in pure water, the one in 80% aqueous ethanol exhibited a significantly higher percentage of small particles, as suggested by the peak areas. Further study revealed that this percentage increased gradually from 20% in pure water to 60% in 80% ethanol (Figure 2C), and the trend was the same at all protein concentrations investigated. Besides, the total number of particles could be estimated indirectly from the count rate, the cumulative light pulses of the sample over the duration of the DLS experiment.[6] The count rate is proportional to the concentration of particles, but it also varies as the sixth power of their size, according to the Rayleigh scattering theory. Assuming the particle numbers were equal, because the particle size of the SPI dispersion in 80% ethanol was approximately 33% of that with 40% ethanol (Figure 1A), the count rate of the former one should have been less than 0.15% (0.33^6) of that with the latter one. However, the count rate actually increased nearly 3-fold as the ethanol concentration increased from 40% to 80% (Table 1), which implied an extensive increase in the number of particles. Moreover, the turbidity of the dispersion increased significantly as the ethanol concentration increased from 40% to 80% (data not shown), which also suggested the existence of aggregates in large quantity.[28,29] These results, combined with the size distribution, indicated a rapid increase in both the number and the percentage of small particles. In addition, because of the overwhelming increase in the total number, the count of the large aggregates might also have increased, although not as rapidly as the small ones. As inferred from the above discussion, the apparently smaller particle sizes observed in 80% ethanol was probably due to the extensive formation of new particles, especially the small ones, rather than the breakdown of large aggregates.

The zeta potential of SPI/water dispersion ranged from −43.2 mV to −34.7 mV, depending on the protein concentrations. The zeta potential decreased (in terms of

dx.doi.org/10.1021/jf205238x | J. Agric. Food Chem. 2012, 60, 2712−2720

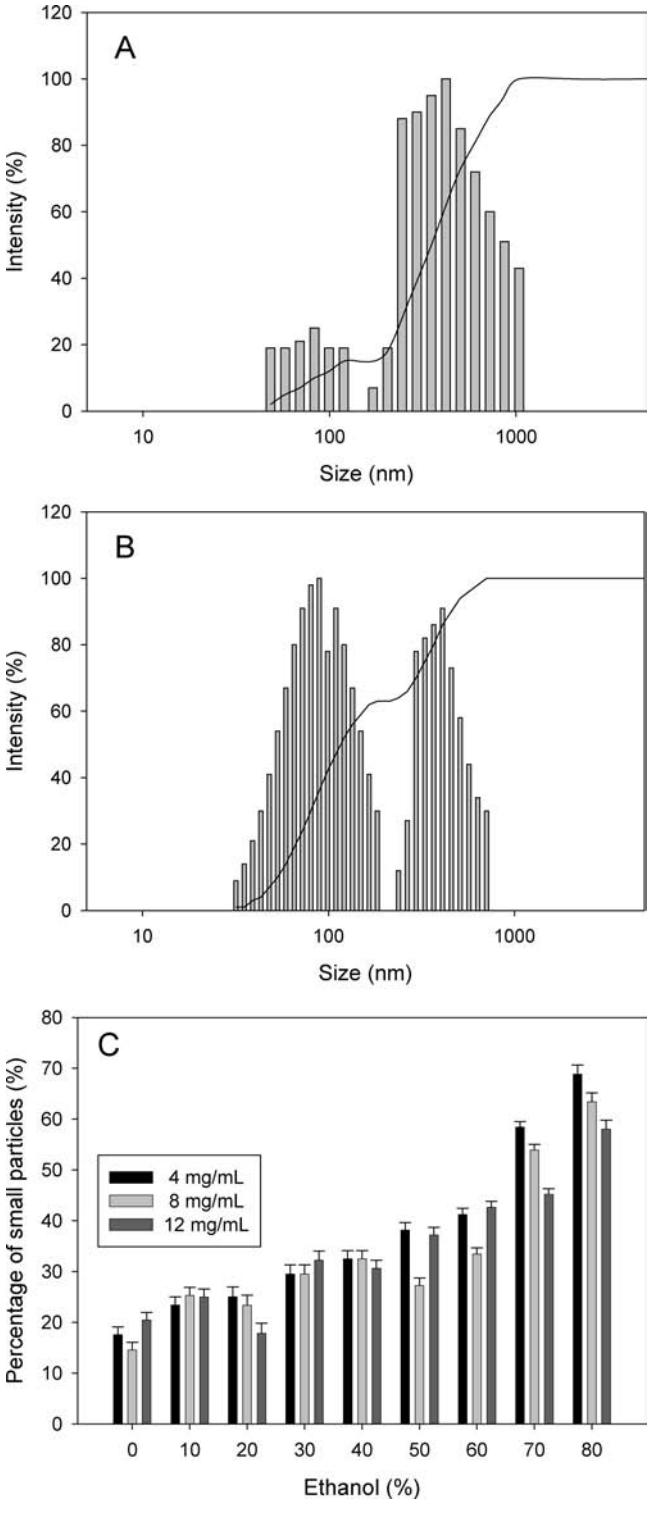

Figure 2. Size distributions of soy protein nanoparticles formed with 8 mg/mL SPI in (A) pure water or (B) 80% ethanol. Panel C shows the effect of ethanol concentration on the percentage of the small particles with average sizes of around 100 nm.

absolute value, similarly hereinafter) with increasing ethanol concentration and reached a minimum value of −8.3 mV at 80% ethanol. This phenomenon was possibly due to the deprivation of water by ethanol that impaired the ionization of the charged groups in soy protein molecules.[24] It was noteworthy that the zeta potential continued decreasing as ethanol concentration increased from 40% to 80%. As a result, the electrostatic repulsion among protein molecules was weakened, thus promoting the formation of protein aggregates and preventing their dissociation.[18] This was supportive for the above discussion on the behavior of soy protein at high ethanol concentrations.

Table 1. Effect of Ethanol on the Count Rate of Soy Protein Nanoparticle Dispersion[a]

EtOH%	count (kcps)	EtOH%	count (kcps)
0	110 ± 15^{e}	50	200 ± 13 ^{cd}
10	120 ± 10de	60	250 ± 19 ^{c}
20	140 ± 20^{d}	70	320 ± 18 ^{b}
30	165 ± 13^{d}	80	550 ± 17 ^{a}
40	140 ± 16^{d}		

[a]Data with different letters showed significant difference (n = 3, P < 0.05).

Effect of Cross-Linking and Evaporation Procedures. Glutaraldehyde is used widely to harden protein nanoparticles or hydrogels as it cross-links the ε-amino groups of lysine residues.[1,3] One treatment (8 mg/mL SPI desolvated by 80% ethanol) was chosen to be further cross-linked by glutaraldehyde, and the effect of cross-linking and evaporation step on the particle size, count rate, and zeta potential was summarized in Figure 3A−C, respectively. Similar results were observed at different protein and ethanol concentrations (data not shown). The sizes were measured after 16 h of cross-linking and were around 200−500 nm, generally higher than those observed immediately after the desolvation without cross-linking (Figure 1A). Before ethanol was evaporated, the particle size appeared independent of the concentration of glutaraldehyde. Similar results were reported on HSA and legumin nanoparticles.[6,30] Besides, the count rates did not change significantly at glutaraldehyde levels lower than 100% equivalent, but it increased by 50% at glutaraldehyde concentrations of 125% and 150% equivalent (Figure 3B). Since the particles sizes exhibited no statistical difference, the increase in count rate indicated that more particles with the same size were formed.[6]

After the removal of ethanol via rotary evaporation, there was a significant increase (P < 0.05) in the particle size and a decrease in count rate at the glutaraldehyde concentrations ranging from 0% to 50% equivalent (Figure 3A,B). These values, as well as the size distribution (data not shown), were similar with those of the particles formed initially without ethanol. In the previous section, increased count rate and decreased average size indicated the extensive formation of small nanoparticles upon the addition of ethanol. Similarly, the reverse change of these values after the removal of ethanol suggested that part of the particles might have dissociated. This might be related to the hydrophilic nature of soy proteins as explained in the introduction section. At glutaraldehyde levels higher than 75% equivalent, however, the particle sizes and count rates did not change significantly after evaporation. This indicated adequate hardening of the soy protein nanoparticles, which is vital for their stability and application in physiological systems.[3] When more than 100% equivalent of glutaraldehyde was added, both the size and count rate increased at a significant level (P < 0.05). On the basis of the result above, it could be inferred that at low concentration glutaraldehyde played a role in maintaining the size and count of existing particles, while at high concentrations, glutaraldehyde contributed to the formation of new particles.

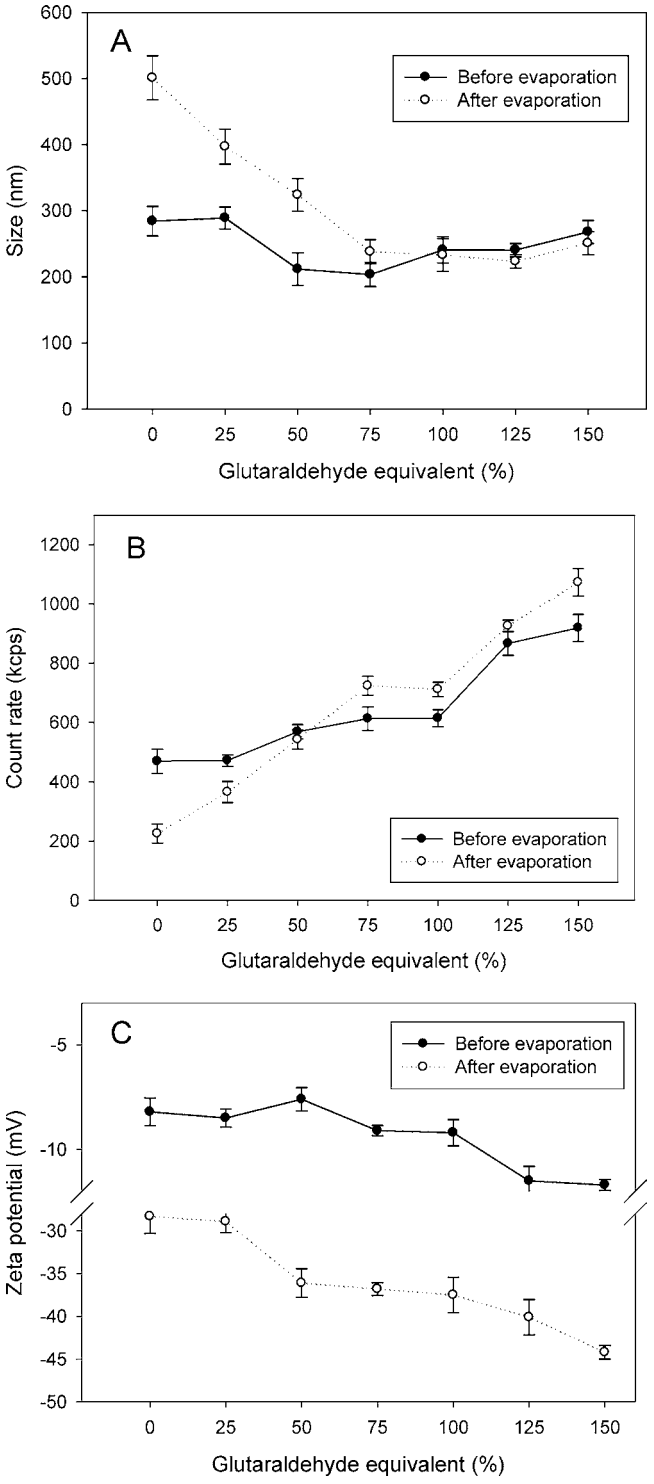

Figure 3. Effect of glutaraldehyde on the size (A), count rate (B), and zeta potential (C) of soy protein nanoparticles after and before evaporation.

Figure 3C displayed the effect of glutaraldehyde on the zeta potential of nanoparticles formed with 8 mg/mL SPI desolvated with 80% ethanol. Before evaporation, the zeta potentials ranged between −7.6 mV and −10.7 mV. According to the American Society for Testing and Materials, these values indicated "incipient instability" of the nanoparticle dispersions,[31] which was in consistence with the emergence of minor flocculates. After ethanol was evaporated, the zeta potential increased to −28.3 mV or −44.2 mV in the presence of 0% or 150% equivalent of glutaraldehyde, respectively. These data were indicative for "moderate to good" stability.[31] The removal of organic solvent increased the polarity of the dispersion, which might have facilitated the electrolysis of protein molecules and increased the zeta potential consequently. In addition, higher glutaraldehyde concentrations resulted in more negative zeta potentials, probably because of the consumption of positively charged ε-amino groups during the cross-linking process.[6]

Encapsulation of Curcumin into SPI Nanoparticles. Table 2 presented the EE, LE, particle size, and zeta potential of blank and curcumin-loaded SPI nanoparticles. The EE increased with decreasing curcumin/protein (C/P) ratios and reached 97.2% at the C/P ratio of 1/100. The maximum LE achieved in this study was 2.7%, which was approximately 40% lower than the one attained with zein nanoparticles.[12] In comparison with soy protein, zein exhibited a higher hydrophobicity, which might have contributed to the protein−curcumin interaction and yielded a higher LE.[13,32] Furthermore, a considerable amount of caseinate was added with the zein nanoparticles (zein: caseinate = 1.25:1, w/w) as a stabilizer,[12] which might further facilitate the encapsulation of curcumin in zein nanoparticles.

Table 2. Characteristics of Blank and Curcumin-Loaded Soy Protein Nanoparticles[a]

curcumin/protein ratio	encapsulation efficiency (%)	loading efficiency (%)	particle size (nm)	zeta potential (mV)
0 (pure SPI)			201.5 ± 9.2[c]	−36.8 ± 1.0[a]
1.00%	97.2 ± 2.0[a]	1.1 ± 0.1[c]	220.1 ± 17.8[b]	−36.0 ± 2.1[a]
2.00%	81.2 ± 1.2[a]	1.7 ± 0.1[b]	252.6 ± 13.4[ab]	−35.2 ± 0.8[a]
5.00%	52.8 ± 3.0[b]	2.7 ± 0.2[a]	286.7 ± 10.1[a]	−34.5 ± 1.4[a]

[a]Data with different letters showed significant difference (n = 3, P < 0.05).

The sizes and zeta-potentials of blank and curcumin-loaded SPI nanoparticles were measured after the encapsulation procedures. As shown in Table 2, the size of blank nanoparticles averaged at 201.5 nm, and it increased with the C/P ratio to a maximum of 286.7 nm. The zeta potentials of blank and curcumin-loaded nanoparticles were around −35 mV with no significant difference. Similar results were reported by Ashok et al. who studied the curcumin-loaded zein nanoparticles.[12] Curcumin possesses four ionizable protons and exhibited a zeta potential of around −6 mV in ethanol or Tween 20/water as measured in our study. Therefore, curcumin was unlikely to interact electrostatically with the negatively charged soy proteins, and the zeta potential of the nanoparticle dispersion was thus not influenced by the presence of curcumin.

FT-IR Study. The FT-IR spectra of SPI, curcumin, their physical mixture (S/C Mix, SPI: curcumin=40:1) and curcumin-loaded nanoparticles (S/C Encap, SPI: encapsulated curcumin=39:1) were presented in Figure 4A. The characteristic peaks of SPI[33] were amide I (band a, C═O stretching, 1637 cm^{-1}), amide II (band b, N−H bending, 1536 cm^{-1}), symmetric COO^- stretching (band c, 1450 cm^{-1}) amide III (band d, C−H vibration in peptide bonds, 1238 cm^{-1}). On the other hand, CUR exhibited several absorbance peaks,[34] of which three were also observed in the S/C mixture: band e, C−

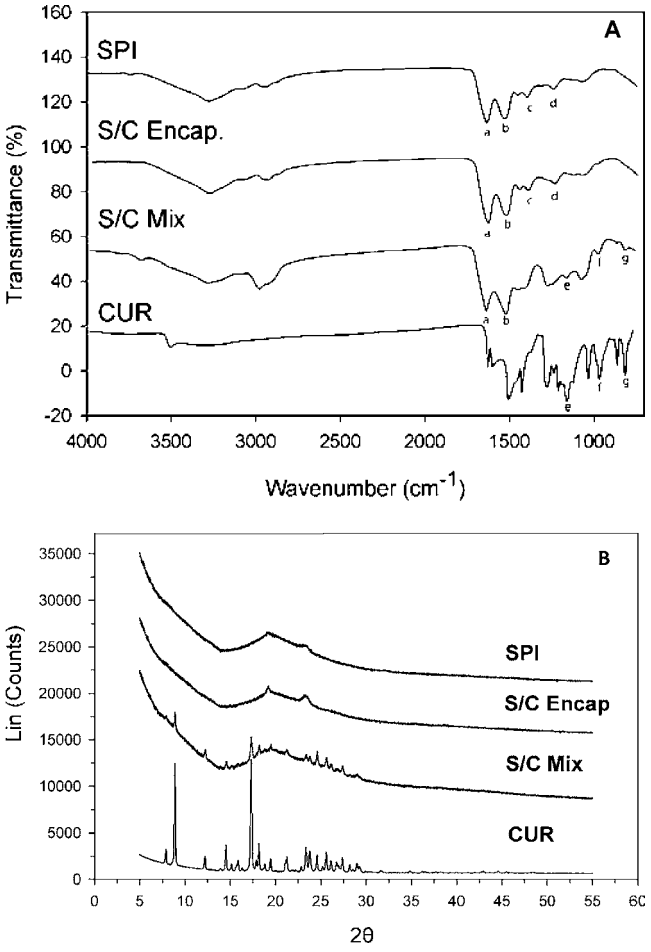

Figure 4. FT-IR spectra (A) and XRD patterns (B) of soy protein isolate (SPI), curcumin (CUR), their physical mixture (S/C Mix), and curcumin-loaded SPI nanoparticles (S/C Encap).

O stretching, 1206 cm^{-1}, band f, trans CH═CH stretching, 1026 cm^{-1}, and band g, C−O−C asymmetric stretching, 856 cm^{-1}. The spectrum of S/C Encap, however, nearly overlapped with that of SPI, and none of these three peaks was detected. This phenomenon indicated that no or little amount of curcumin existed in S/C Encap as free molecules,[35,36] which will be confirmed by the results of SEM.

XRD Analysis. Figure 4B showed the XRD patterns of SPI, curcumin, their physical mixture (S/C Mix, SPI: curcumin = 40:1), and curcumin-loaded nanoparticles (S/C Encap, SPI: curcumin = 39:1). The characteristic peaks of curcumin at 8.84, 12.10, 14.39, 17.20, 23.33, 24.50, 25.52, and 28.87° suggested its highly crystalline nature, which was consitent with previous literatures.[12] These peaks were also observed in the S/C Mix, but with significantly lower intensities. On the contrast, these peaks disappeared in the XRD pattern of S/C Encap, which consisted mostly of amorphous humps. These results indicated the successful incorporation of curcumin in the nanoscale SPI matrix, which facilitated the conversion of crystalline curcumin into an amorphous state.[12,37]

SEM Analysis of the Blank and Curcumin-Loaded Nanoparticles. The morphology of blank and curcumin-loaded SPI nanoparticles was investigated under SEM. When 12 mg/mL of SPI was dispersed in pure water (Figure 5A), a film-like structure was observed under SEM. Similar images were obtained when the same concentration of SPI was desolvated with 80% ethanol without cross-linking (not shown). This structure was possibly formed by nonparticulate soy proteins that attached each other during the drying process.[8] Intermolecular attraction and hydrophobic interaction might have played a role in the formation of the network structure.[38] After cross-linking was performed with 75% equivalent of glutaraldehyde, the proportion of particulate soy protein appeared to increase significantly (Figure 5B). The particles exhibited an approximately spherical shape with a smooth surface. The particle size under SEM ranged from 50 to 200 nm, which was about 30% lower than the values obtained by DLS. This difference was probably due to the shrinkage caused by the cast-drying process as well as the vacuum environment in SEM imaging.[30]

After the removal of ethanol by rotary evaporation, the particles tended to separate from each other (Figure 5C). This result could be attributed to the increased polarity of the solvent, which induced the burial of hydrophobic chains of protein molecules.[27] In addition, the nanoparticles carried more negative charges on the surface after the evaporation as discussed before. These two factors led to strengthened electrostatic repulsion and weakened hydrophobic interaction among protein nanoparticles, both of which inhibited the association of particles upon drying. After the incorporation of curcumin, clusters of individual particle units were formed with particles (Figure 5D), which was responsible for the aforementioned increase in particle sizes. No curcumin crystal (as shown in Figure 5E) was observed in the curcumin-loaded particles, suggesting the burial of curcumin into the protein matrix.

Release of Curcumin from SPI Nanoparticles. Figure 6 showed the kinetic release profiles of curcumin from SPI nanoparticles in the PBS/Tween 20 system. A biphasic trend was observed for the samples with different C/P ratios, namely, from 1/100, 2/100, and 5/100. In the first 1.5 h, over 50% of the encapsulated curcumin was released for all formulations. This phenomenon of burst effect was due to the swelling and breakage of the protein matrix.[23] In addition, the majority of curcumin that was initially bound to the peripheral domain of the protein matrix might have migrated to the releasing medium during the first 1.5 h.[7] Similar results have been reported on the nanoparticles prepared with different proteins, such as albumin[10] and zein.[12] Possible strategies for reducing the burst effect include chemical modification of proteins, optimization of encapsulation procedure, and preparation of multilayer encapsulation systems with protein and polysaccharides, such as chitosan derivatives.[39,40] Between hours 2 and 8, a sustained release phase was observed in which the concentration of released curcumin increased slowly with time. At the end of 8 h, the total percentage of curcumin released ranged from 58% to 78%, and it continued to increase in the following 24 h (data not shown). These results correspond to the migration of curcumin encapsulated within the hydrophobic core of protein molecules. In addition, nanoparticles with lower C/P ratio exhibited higher releasing rates in the PBS/Tween 20 system. This was probably due to their smaller sizes and greater area-to-volume ratios, which facilitated the contact with the releasing medium.[41]

Proposed Mechanism of Nanoparticle Preparation and Encapsulation. On the basis of the results obtained in previous sections, an illumination for the formation of blank and curcumin-loaded SPI nanoparticles was proposed in Figure 7. When dispersed in pure water (phase 1), soy protein existed

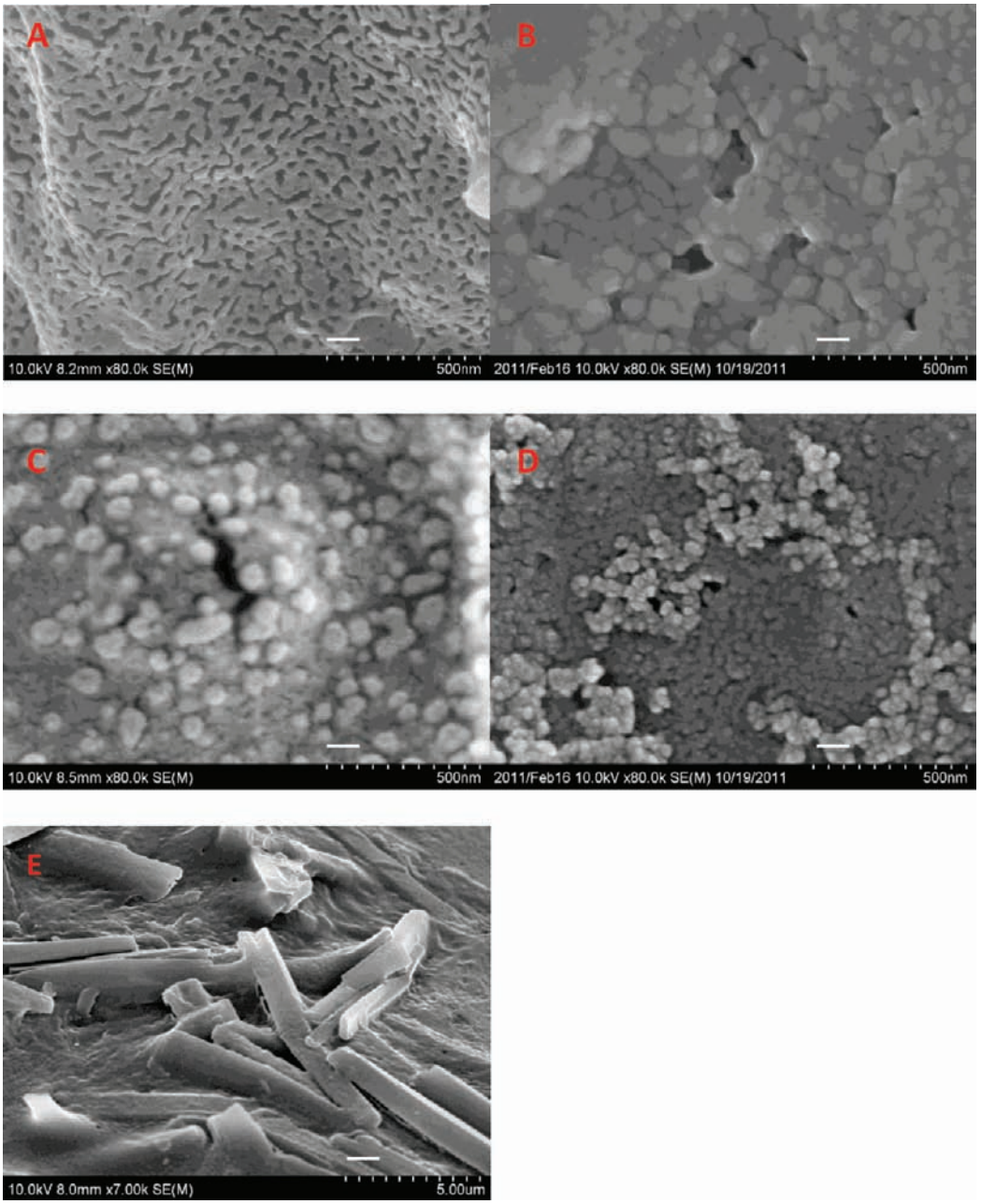

Figure 5. SEM images of soy protein nanoparticle dispersions formed by (A) 12 mg/mL soy protein isolate in pure water, (B) 12 mg/mL protein and 80% ethanol with 75% equivalent of glutaraldehyde, (C) same formula as B after ethanol removal, and (D) same formula as C, loaded with 0.6 mg/mL curcumin. Panel E shows the crystal formed with pure curcumin. The white bars in panels A–D represent 100 nm, while the bar in panel E represents 1 μm.

mostly in its native state, i.e., globular molecules consisting of a shell of charged or polar groups together with a kernel formed by hydrophobic chains.[18,38] There existed a small amount of aggregates, especially the large ones with diameters of 500–1000 nm. When ethanol was added to the concentration of 40%, the hydration and electrolysis of protein were disturbed, leading to a decrease in the zeta potential (phase 2). Meanwhile, part of the hydrophobic chains were exposed to the surface of the molecule.[18] As a consequence, the attraction among protein molecules was enhanced, and a relatively small amount of protein aggregate began to form, resulting in an increase in the average particle size. As shown in our study, the desolvation process could be partly reversed if ethanol was evaporated at this point. Then, curcumin–ethanol solution was added to achieve an ethanol concentration of 50–60%, so that (a) curcumin could disperse well without agglomeration, (b) the hydrophobic chain of protein was further exposed, and (c) extensive aggregation of protein did not occur and the hydrophobic sites in soy protein molecules were not consumed completely for protein–protein interaction (phase 3). Thereafter, the concentration of ethanol was increased to 80% (with 8–12 mg/mL SPI), which led to an extensive formation of nanoparticles, especially those with smaller sizes (50–200 nm). At this stage, part of curcumin was entrapped inside the protein particles, while some curcumin molecules were bound to their peripheral domains (as illustrated in the figure). There was also a certain amount of the drug existing as freely dissolved molecules. After adequate hardening by glutaraldehyde,

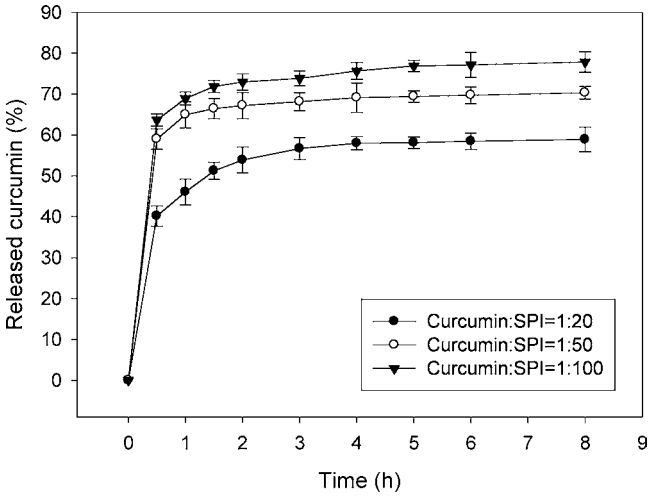

Figure 6. Release of curcumin from the soy protein nanoparticles in phosphate buffer saline with Tween 20.

sufficient amide bonds were formed to prevent the deformation of the particles (phase 4). Therefore, the size and number of the particles was not changeable upon the removal of ethanol. However, the constituent part of the nanoparticles, either protein monomers or oligomers, was prone to adopting their native core−shell conformation (phase 5). This was speculated from the fact that the zeta potential of the nanoparticles after ethanol removal was close to that of the SPI dispersion before desolvation took place. In addition, as was discussed before, the results on SEM images before and after evaporation also suggested the burial of hydrophobic chains and the exposure of polar and charged sites. In addition, the removal of ethanol resulted in an increased polarity of the dispersion, which favored thermodynamically the hydrophobic interaction (a) among curcumin molecules and (b) between curcumin and the nonpolar groups of the protein. The former interaction might have caused the precipitation of the unbound curcumin,[8] while the latter one facilitated the entrapment of curcumin into the protein matrix.[7,11] As a result, little or no curcumin existed in the final product as freestanding molecules.

Conclusions. Nanoparticles were successfully synthesized with SPI using a desolvation method. An ethanol concentration greater than 80% was required for extensive formation of particles, while more than 75% equivalent of glutaraldehyde was necessary for adequate hardening. The zeta potential of the nanoparticle dispersion was around −36 mV, which indicated moderate to good stability. The synthesized nanoparticles exhibited an approximate spherical structure with a smooth surface. These particles were then evaluated for their encapsulating capability, and a highest encapsulation efficiency of 97.2% was achieved. No or little curcumin existed as unbound molecules in the yielded particles, as was supported by FT-IR and XRD results. The release of curcumin in PBS/Tween 20 system followed a biphasic trend, and the releasing rate varied with the C/P ratio. Nanoparticles prepared from SPI exhibited satisfactory encapsulating properties and a desirable stability at high concentrations, owing to the balanced composition of amino acids. These properties made SPI nanoparticles a promising candidate as a delivery system for drugs or nutraceuticals.

AUTHOR INFORMATION

Corresponding Author

*Tel: (301)-405-8421. Fax: (301)-314-3313. E-mail: wangqin@umd.edu.

Notes

The authors declare no competing financial interest.

ACKNOWLEDGMENTS

We appreciate the support of the Maryland NanoCenter of the University of Maryland in scanning electron microscopy.

REFERENCES

(1) Chen, L. Y.; Remondetto, G. E.; Subirade, M. Food protein-based materials as nutraceutical delivery systems. *Trends Food Sci. Technol.* **2006**, *17* (5), 272−283.

(2) Marty, J. J.; Oppenheim, R. C.; Speiser, P. Nanoparticles: New colloidal drug delivery system. *Pharm. Acta Helv.* **1978**, *53* (1), 17−23.

(3) Jahanshahi, M.; Babaei, Z. Protein nanoparticle: A unique system as drug delivery vehicles. *Afr. J. Biotechnol.* **2008**, *7* (25), 4926−4934.

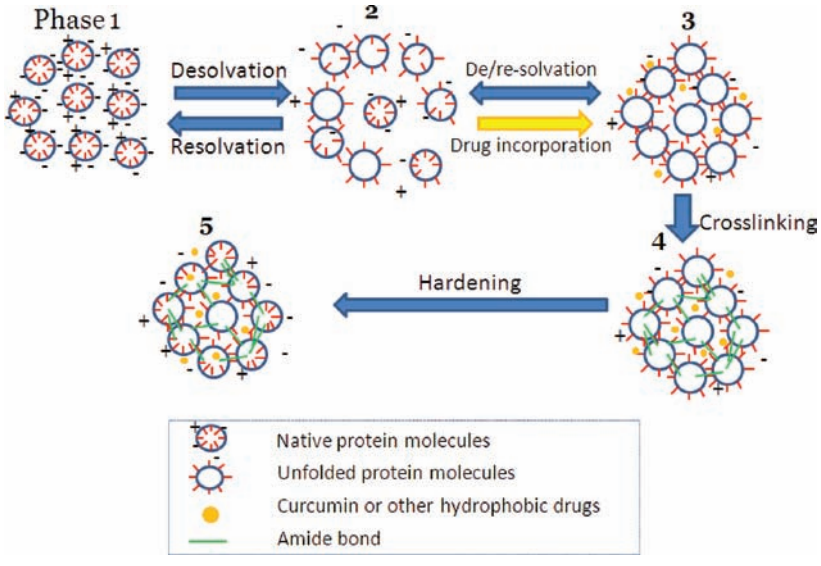

Figure 7. Proposed mechanism of the formation of soy protein nanoparticles.

(4) Kawashima, Y. Nanoparticulate systems for improved drug delivery. *Adv. Drug Delivery Rev.* **2001**, *47* (1), 1−2.
(5) Desai, M. P.; Labhasetwar, V.; Walter, E.; Levy, R. J.; Amidon, G. L. The mechanism of uptake of biodegradable microparticles in Caco-2 cells is size dependent. *Pharm. Res.* **1997**, *14* (11), 1568−1573.
(6) Weber, C.; Coester, C.; Kreuter, J.; Langer, K. Desolvation process and surface characterisation of protein nanoparticles. *Int. J. Pharm.* **2000**, *194* (1), 91−102.
(7) Ezpeleta, I.; Irache, J. M.; Stainmesse, S.; Chabenat, C.; Gueguen, J.; Popineau, Y.; Orecchioni, A. M. Gliadin nanoparticles for the controlled release of all-trans-retinoic acid. *Int. J. Pharm.* **1996**, *131* (2), 191−200.
(8) Zhong, Q. X.; Jin, M. F. Zein nanoparticles produced by liquid−liquid dispersion. *Food Hydrocolloids* **2009**, *23* (8), 2380−2387.
(9) Zu, Y. G.; Zhang, Y.; Zhao, X. H.; Zhang, Q.; Liu, Y.; Jiang, R. Optimization of the preparation process of vinblastine sulfate (VBLS)-loaded folate-conjugated bovine serum albumin (BSA) nanoparticles for tumor-targeted drug delivery using response surface methodology (RSM). *Int. J. Nanomed.* **2009**, *4*, 321−333.
(10) Jithan, A.; Madhavi, K.; Prabhakar, K.; Madhavi, M. Preparation and characterization of albumin nanoparticles encapsulating curcumin intended for the treatment of breast cancer. *Int. J. Pharm. Invest.* **2011**, *1* (2), 119−125.
(11) Luo, Y.; Zhang, B.; Whent, M.; Yu, L.; Wang, Q. Preparation and characterization of zein/chitosan complex for encapsulation of α-tocopherol, and its in vitro controlled release study. *Colloids Surf., B* **2011**, *85* (2), 145−152.
(12) Patel, A.; Hu, Y. C.; Tiwari, J. K.; Velikov, K. P. Synthesis and characterisation of zein−curcumin colloidal particles. *Soft Matter* **2010**, *6* (24), 6192−6199.
(13) Riche, M.; Williams, T. N. Apparent digestible protein, energy and amino acid availability of three plant proteins in Florida pompano, *Trachinotus carolinus L.* in seawater and low-salinity water. *Aquacult. Nutr.* **2010**, *16* (3), 223−230.
(14) Liu, D. G.; Tian, H. F.; Zeng, J.; Chang, P. R. Core-shell nanoblends from soy protein/polystyrene by emulsion polymerization. *Macromol. Mater. Eng.* **2008**, *293* (8), 714−721.
(15) Yu, L. W.; Yan, D. Y.; Sun, G.; Gu, L. X. Preparation and characterization of pH-sensitive hydrogel fibers based on hydrolyzed-polyacrylonitrile/soy protein. *J. Appl. Polym. Sci.* **2008**, *108* (2), 1100−1108.
(16) Teng, Z.; Liu, C.; Yang, X. Q.; Li, L.; Tang, C. H.; Jiang, Y. M. Fractionation of soybean globulins using Ca(2+) and Mg(2+): A comparative analysis. *J. Am. Oil Chem. Soc.* **2009**, *86* (5), 409−417.
(17) Utsumi, S.; Kinsella, J. E. Structure−function relationships in food proteins: subunit interactions in heat-induced gelation of 7S, 11S, and soy isolate proteins. *J. Agric. Food Chem.* **1985**, *33* (2), 297−303.
(18) Li, X. H.; Li, Y.; Hua, Y. F.; Qiu, A. Y.; Yang, C.; Cui, S. Effect of concentration, ionic strength and freeze-drying on the heat-induced aggregation of soy proteins. *Food Chem.* **2007**, *104* (4), 1410−1417.
(19) Lazko, J.; Popineau, Y.; Legrand, J. Soy glycinin microcapsules by simple coacervation method. *Colloids Surf., B* **2004**, *37* (1−2), 1−8.
(20) Jong, L.; Peterson, S. C. Effects of soy protein nanoparticle aggregate size on the viscoelastic properties of styrene−butadiene composites. *Composites, Part A* **2008**, *39* (11), 1768−1777.
(21) Petruccelli, S.; Anon, M. C. Thermal aggregation of soy protein isolates. *J. Agric. Food Chem.* **1995**, *43* (12), 3035−3041.
(22) Marty, J. J.; Oppenheim, R. C.; Speiser, P. Nanoparticles: A new colloidal drug delivery system. *Pharm. Acta Helv.* **1978**, *53* (1), 17−23.
(23) Hu, B.; Pan, C. L.; Sun, Y.; Hou, Z. Y.; Ye, H.; Hu, B.; Zeng, X. X. Optimization of fabrication parameters to produce chitosan−tripolyphosphate nanoparticles for delivery of tea catechins. *J. Agric. Food Chem.* **2008**, *56* (16), 7451−7458.
(24) Malhotra, A.; Coupland, J. N. The effect of surfactants on the solubility, zeta potential, and viscosity of soy protein isolates. *Food Hydrocolloids* **2004**, *18* (1), 101−108.
(25) Phianmongkhol, A.; Varley, J. ζ-potential measurement for air bubbles in protein solutions. *J. Colloid Interface Sci.* **2003**, *260* (2), 332−338.
(26) Fukushima, D. Denaturation of soybean proteins by organic solvents. *Cereal Chem.* **1969**, *46* (2), 156−63.
(27) Kavanagh, G. M.; Clark, A. H.; Ross-Murphy, S. B. Heat-induced gelation of globular proteins: part 3. Molecular studies on low pH beta-lactoglobulin gels. *Int. J. Biol. Macromol.* **2000**, *28* (1), 41−50.
(28) Dao, L. H.; Nguyen, H. M.; Mai, H. H. A fiber optic turbidity system for in-situ monitoring protein aggregation, nucleation and crystallisation. *Acta Astronaut.* **2000**, *47* (2−9), 399−409.
(29) LaClair, C. E.; Etzel, M. R. Turbidity and protein aggregation in whey protein beverages. *J. Food Sci.* **2009**, *74* (7), C526−C535.
(30) Mirshahi, T.; Irache, J. M.; Gueguen, J.; Orecchioni, A. M. Development of drug delivery systems from vegetal proteins: Legumin nanoparticles. *Drug Dev. Ind. Pharm.* **1996**, *22* (8), 841−846.
(31) Zeta Potential of Colloids in Water and Waste Water. In *ASTM Standard D*; American Society for Testing and Materials: West Conshohocken, PA, 1985; pp 4187−82.
(32) Gianazza, E.; Viglienghi, V.; Righetti, P. G.; Salamini, F.; Soave, C. Amino acid composition of zein molecular components. *Phytochemistry* **1977**, *16* (3), 315−17.
(33) Liu, Y. Y.; Zeng, X. A.; Deng, Z.; Yu, S. J.; Yamasaki, S. Effect of pulsed electric field on the secondary structure and thermal properties of soy protein isolate. *Eur. Food Res. Technol.* **2011**, *233* (5), 841−850.
(34) Zaibunnisa, A. H.; Siti Rashima, R.; Nur Ain, A. H., Stabilisation of Curcumin With γ-Cyclodextrin: Phase Solubility Study and its Characterisation. In *2nd International Conference on Biotechnology and Food Science*; IACSIT Press: Singapore, 2011; Vol. 7, pp 9−13.
(35) Sahu, A.; Kasoju, N.; Goswami, P.; Bora, U. Encapsulation of curcumin in pluronic block copolymer micelles for drug delivery applications. *J. Biomater. Appl.* **2011**, *25* (6), 619−639.
(36) Paramera, E. I.; Konteles, S. J.; Karathanos, V. T. Microencapsulation of curcumin in cells of Saccharomyces cerevisiae. *Food Chem.* **2011**, *125* (3), 892−902.
(37) Shaikh, J.; Ankola, D. D.; Beniwal, V.; Singh, D.; Kumar, M. N. V. R. Nanoparticle encapsulation improves oral bioavailability of curcumin by at least 9-fold when compared to curcumin administered with piperine as absorption enhancer. *Eur. J. Pharm. Sci.* **2009**, *37* (3−4), 223−230.
(38) Caillard, R.; Remondetto, G. E.; Subirade, M. Physicochemical properties and microstructure of soy protein hydrogels co-induced by Maillard type cross-linking and salts. *Food Res. Int.* **2009**, *42* (1), 98−106.
(39) McClements, D.; Decker, E.; Park, Y.; Weiss, J. Designing food structure to control stability, digestion, release and absorption of lipophilic food components. *Food Biophys.* **2008**, *3* (2), 219−228.
(40) Luo, Y.; Teng, Z.; Wang, Q. Development of zein nanoparticles coated with carboxymethyl chitosan for encapsulation and controlled release of vitamin D3. *J. Agric. Food Chem.* **2012**, *60* (3), 836−843.
(41) Patel, K.; Patel, V.; Patel, M.; Patel, P.; Ajmera, A.; Rathod, K. Preparation and characterization of Tramadol hydrochloride microspheres. *Int. J. Drug Dev. Res.* **2010**, *2* (3), 605−611.